ЖЭТФ, 2002, том 122, вып. 4 (10), стр. 849–862

PRESSURE-INDUCED TRANSFORMATIONS AND OPTICAL PROPERTIES OF THE TWO-DIMENSIONAL TETRAGONAL POLYMER OF C_{60} AT PRESSURES UP TO 30 GPa

K. P. Meletov *

Institute of Solid State Physics, Russian Academy of Sciences
142432, Chernogolovka, Moscow Region, Russia

J. Arvanitidis, S. Assimopoulos, G. A. Kourouklis

Physics Division, School of Technology, Aristotle University of Thessaloniki
GR-540 06, Thessaloniki, Greece

B. Sundqvist

Department of Physics, Umeå University
S-901 87, Umeå, Sweden

Submitted 24 April 2002

The Raman spectra of the two-dimensional tetragonal ($2D$(T)) polymeric phase of C_{60} have been studied *in-situ* at pressures up to 30 GPa and room temperature. The pressure dependence of the phonon modes shows an irreversible transformation of the material near 20 GPa into a new phase, most probably associated with the covalent bonding between the $2D$ polymeric sheets. The Raman spectrum of the high-pressure phase is intense and well-resolved and the majority of modes are related to the fullerene molecular cage. The sample recovered at ambient conditions is in a metastable phase and transforms violently under laser irradiation: the transformed material contains mainly dimers and monomers of C_{60} and small inclusions of the diamond-like carbon phase. The photoluminescence spectra of the $2D$(T) polymer of C_{60} were measured at room temperature and pressure up to 4 GPa. The intensity distribution and the pressure-induced shift of the photoluminescence spectrum drastically differ from those of the C_{60} monomer. The deformation potential and the Grüneisen parameters of the $2D$(T) polymeric phase of C_{60} have been determined and compared with those of the pristine material.

PACS: 61.48.+c, 62.50.+p, 64.70.Kb, 78.30.Na, 78.55.Kz

1. INTRODUCTION

The polymeric forms of C_{60} have attracted considerable attention because of their interesting structure and properties [1]. Pristine C_{60} has a great potential for polymerization because of the existence of 30 double C═C bonds in the fullerene molecular cage. C_{60} has been found to polymerize under illumination with visible and ultraviolet light [2] and upon alkali metal doping [3, 4]. The treatment of C_{60} under various high-pressure and high-temperature conditions also leads to polymerization of the material (HPHT polymers) [5]. The covalent polymeric bonds are usually formed by the so-called [2 + 2] cyclo-addition reaction via the formation of four-member rings between adjacent fullerene molecules, resulting in an appreciable decrease of the intermolecular distance [2].

The structure and the dimensionality of HPHT polymers strongly depend on the pressure (P) and temperature (T) treatment conditions. The C_{60} molecules form linear polymeric chains (one-dimensional polymer) having an orthorhombic crystal structure ($1D$(O)) and/or dimers and higher oligomers at lower P and T, two-dimensional polymeric layers that have either a rhombohedral ($2D$(R)) or a tetragonal ($2D$(T)) crystal structure at intermediate P and T, and face-centered cubic structures based on three-dimensionally ($3D$) cross-linked polymerization of the material at higher

*E-mail: mele@issp.ac.ru

P and T [1, 5–7]. In addition, the treatment of the pristine material under high nonuniform pressure and high temperature leads to the creation of several disordered polymeric phases, the so-called ultrahard fullerite phases [8, 9]. The detailed X-ray studies of these phases have revealed their $3D$ polymeric character [10, 11].

The polymerization of C_{60} is characterized by the destruction of a number of double C═C intramolecular bonds and the creation of intermolecular covalent bonds associated with sp^3-like fourfold coordinated carbon atoms in the fullerene molecular cage. Their number increases from 4 to 8 and to 12 per each cage for $1D$(O), $2D$(T), and $2D$(R) polymeric phases, respectively, and is expected to further increase in the $3D$ polymeric phases. Theoretical studies by Okada et al. [12] have predicted that the $3D$-polymerized C_{60} might be formed by the application of uniaxial pressure perpendicular to the polymeric sheets of the $2D$(T) phase of C_{60}. According to their density-functional calculations, polymerization occurs at the lattice constant $c = 10.7$ Å, which is attainable at the pressure of approximately 20.2 GPa. This polymerization results in the formation of a stable metallic phase having 24 sp^3-like and 36 sp^2-like hybridized carbon atoms in each C_{60} molecule. Another theoretical study, by Burgos et al. [13], predicted that uniaxial compression perpendicular to the chains in the $1D$ or to the polymeric planes in the $2D$ polymeric phases of C_{60} leads to $3D$ polymerization with 52, 56, and even 60 sp^3-like coordinated carbon atoms per C_{60} molecular cage. These transformations are expected to occur at pressures lower than 14 GPa, and the new phases are semiconducting with large bulk and shear moduli.

The Raman scattering and infrared absorption spectra of various polymeric phases prepared under carefully controlled conditions of HPHT treatment have a very rich and prominent structure. Their intensity distribution and peak positions differ significantly for the $1D$(O), $2D$(R), and $2D$(T) polymeric phases, as has been shown by the detailed study of their optical spectra combined with their structural analysis [14]. The phonon spectra of these materials are very sensitive to any perturbation of the fullerene molecular cage caused by external disturbances such as pressure or chemical bond formation [15, 16]. Therefore, the Raman spectroscopy can be successfully used for the identification of various polymeric phases of C_{60} and for the *in-situ* high-pressure studies of phase transformations in the fullerene-related materials. Our experimental Raman studies of the pressure dependence of the $2D$(T) polymeric phase of C_{60} [17, 18] have revealed prominent irreversible changes in the Raman spectra of this material near 20 GPa, most probably related to its further polymerization in accordance with the theoretical prediction by Okada et al. [12]. The well-structured phonon spectrum of the new high-pressure phase in the $2D$(T) polymer provides strong indications that the fullerene molecular cage is retained and that the new phase may be related to a three-dimensional network of the C_{60} molecules. The Raman data [17, 18] disagree with the results of recent high-pressure X-ray studies of the $2D$(T) polymer: this fact shows that the material undergoes an irreversible amorphization in the pressure region between 10 and 20 GPa [19]. It is also interesting to note that contrary to the $2D$(T) polymer, the $2D$(R) polymeric phase of C_{60} transforms to a new phase at approximately 15 GPa; this phase is characterized by very diffused Raman bands that are most probably related to the random covalent bonding between molecules belonging to adjacent $2D$ polymeric sheets [20].

In this work, we present a detailed photoluminescence and Raman study of the intramolecular phonon modes and electronic spectrum behavior of the $2D$(T) polymeric phase of C_{60} at high pressure. Our motivation was to study, in detail, the properties and stability of the material in both $2D$(T) and high-pressure induced phases, to obtain the quantitative data on the pressure behavior of the phonon and electron spectra, and to compare them with those of pristine C_{60}.

2. EXPERIMENTAL DETAILS

Two-dimensionally polymerized C_{60} was obtained by subjecting the 99.99 % pure C_{60} powder to the pressure 2.2 GPa at the temperature about 820 K [21]. An X-ray analysis of the samples from the same batch after the high-pressure and high-temperature treatment confirmed that the crystal structure of the polymer is tetragonal (the space group $P4_2mmc$), while a Raman analysis showed the typical spectrum of the $2D$(T) polymer of C_{60} with no detectable inclusions of orthorhombic or rhombohedral phases [14, 21, 22].

Raman spectra were recorded using a triple monochromator (DILOR XY-500) equipped with a CCD liquid-nitrogen cooled detector system. The spectra were taken in the back-scattering geometry using a micro-Raman system comprising an OLYMPUS microscope equipped with objectives of 100× and 20× magnification and the respective spatial resolutions of approximately 1.7 μm and 8 μm. The spectral width of the system was about 5 cm^{-1}. The 514.5-nm line of an Ar^+ laser was used for excitation. The laser power

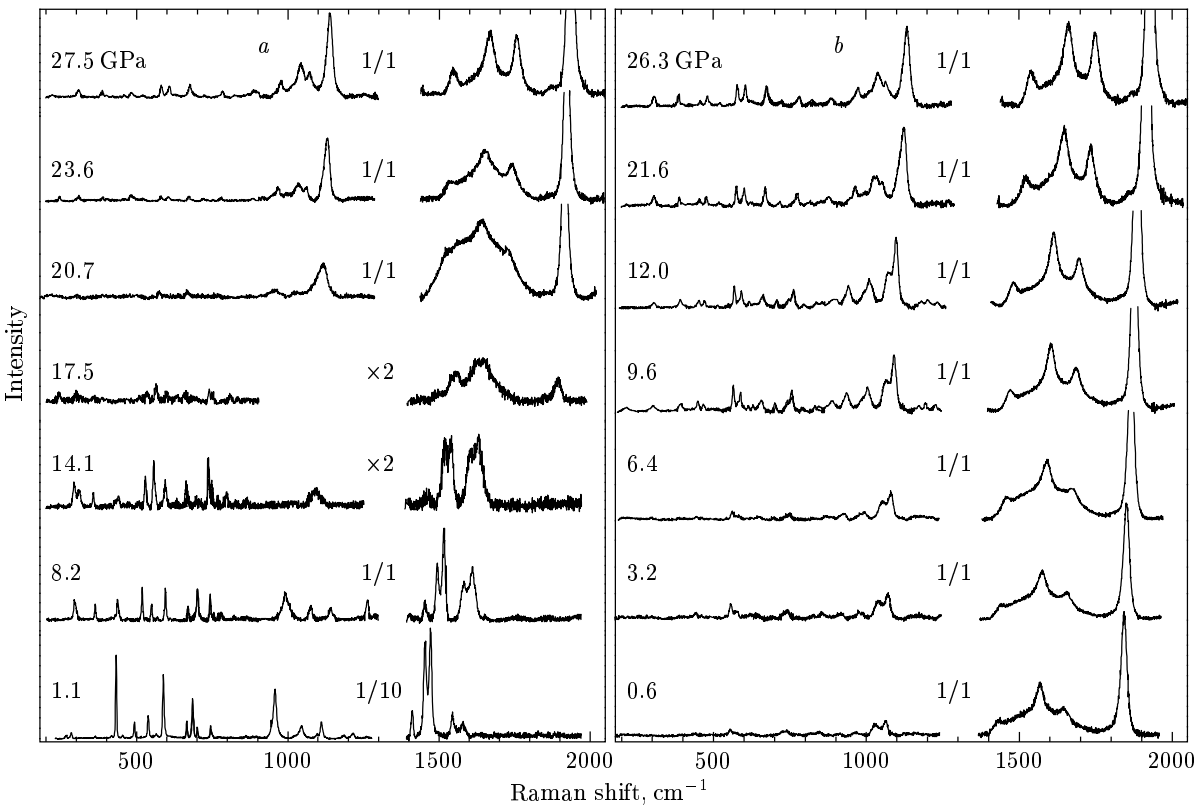

Fig. 1. Raman spectra of the $2D$(T) polymer of C_{60} at 300 K and various pressures, recorded for (a) increasing and (b) decreasing pressure runs. The numbers $1/x$ indicate the relative scale of the spectra

was kept lower than 20 mW measured directly before the high-pressure cell, in order to avoid the destruction of polymeric bonds caused by laser heating effects and related changes in the phonon spectrum and the crystal structure [23–25]. The photoluminescence spectra were recorded using a single monochromator JOBIN YVON THR-1000 equipped with a CCD liquid-nitrogen cooled detector system. The spectral width of the system was approximately 0.5 meV. The 488-nm line of an Ar^+ laser was used for excitation of the luminescence spectra. The laser power was kept at 2 mW measured directly in front of the high-pressure cell.

Measurements of the Raman and photoluminescence spectra at high pressures were carried out using the diamond anvil cell of Mao–Bell type [26]. The 4:1 methanol–ethanol mixture was used as the pressure transmitting medium and the ruby fluorescence technique was used for pressure calibration [27]. The samples used in the present study had dimensions of 100 μm and were selected from the batch material for their intense, clear, and spatially uniform Raman response, typical of the $2D$(T) polymeric phase [14]. The band frequencies in the Raman and photoluminescence spectra were obtained by fitting Lorentzian peak functions to the experimental peaks after the background subtraction.

3. RESULTS AND DISCUSSION

3.1. Phase transitions

The Raman spectra of the $2D$(T) polymer of C_{60} at various pressures up to 27.5 GPa and room temperature, in the frequency region 200–2050 cm^{-1}, are illustrated in Fig. 1a. In this figure, the spectra were recorded upon pressure increase; the spectral region around the strong triple-degenerate T_{2g} mode of diamond appearing at 1332 cm^{-1} at ambient pressure [28] is omitted. The initial spectrum at 1.1 GPa represents a typical Raman spectrum of the $2D$(T) polymeric phase and is identical with the spectra reported earlier [14, 17, 18]. Lowering the molecular symmetry from I_h in pristine C_{60} to D_{2h} in the $2D$(T) polymer results in the splitting of the degenerate icosahedral intramolecular modes and in the activation of ini-

tially silent modes [14, 29, 30]. Moreover, although the $2D$(T) phase retains the inversion center of the pristine C_{60} molecule, we cannot discard the possibility that imperfections in the crystal structure of the polymer and/or the natural ^{13}C substitution may facilitate the appearance of some ungerade modes in its Raman spectrum [30]. For these reasons, the Raman spectrum of the $2D$(T) polymer is richer in structure than that of pristine C_{60} [31].

As can be clearly seen from Fig. 1*a*, the Raman peaks of the $2D$(T) polymer remain narrow and well-resolved for pressures up to 14 GPa, showing the homogeneity and stability of the used samples. We note that as recently shown [30], the pressure behavior of the Raman modes of the $2D$(T) polymer is fully reversible up to 12 GPa. For pressures $P > 14$ GPa, the Raman peak bandwidths of the polymer gradually increased and the intensities of peaks are considerably decreased. In addition, the peak broadening is accompanied by a gradual enhancement of the background (not shown in Fig. 1, because the Raman spectra are presented after the background subtraction). Because the fluorescence from the $2D$(T) polymer of C_{60} appears in another energy region, this background is most probably related to the enhancement of strain and inhomogeneity within the sample induced at higher pressure.

The drastic changes in the Raman spectrum of the $2D$(T) polymer are first observed at $P > 20$ GPa, where new distinct peaks appear in the spectrum and their intensities increase with a further increase of pressure. On the contrary, some of the initial Raman peaks of the polymer disappear above this critical pressure. At $P \geq 20$ GPa, the Raman spectrum of the material is significantly different from the initial one at lower pressure; the observed changes can be attributed to the transition of the polymer to a new high-pressure phase. From Fig. 1*a*, it is clear that even for the applied pressure as high as 27.5 GPa, the Raman spectrum of the high-pressure phase is well resolved with relatively narrow peaks. Moreover, the frequency positions of the majority of the peaks in the new phase can be tracked back to the peaks observed in the initial $2D$(T) polymeric phase of C_{60}. This is a first experimental indication that the C_{60} molecular cages are retained at pressures higher than 20 GPa as the Raman peaks in the high-pressure phase have their origin on intramolecular cage vibrations.

Figure 1*b* shows the Raman spectra of the material upon pressure release. The decrease of pressure from 27.5 GPa to ambient conditions results in the gradual shift of the Raman peaks to lower energies. The release of pressure does not lead to any observable

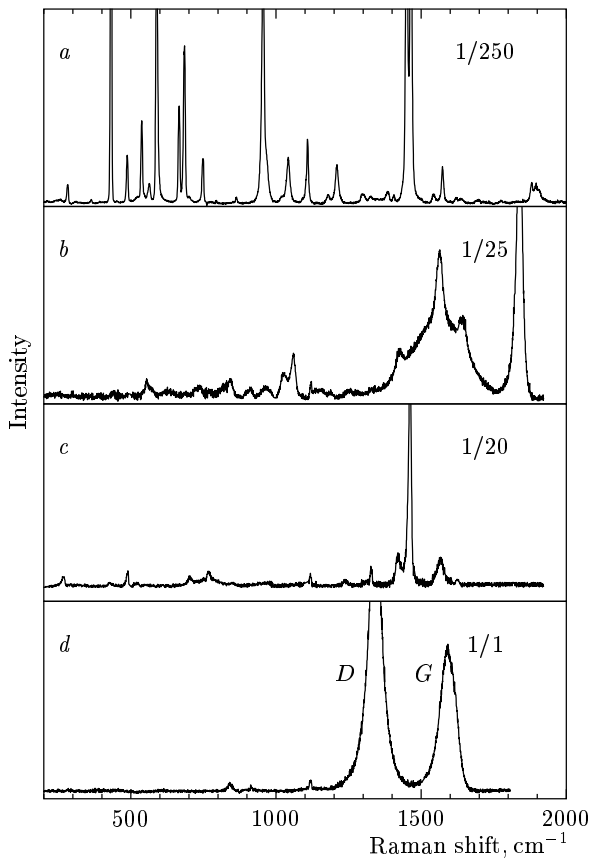

Fig. 2. Raman spectra of the initial $2D$(T) polymer and the recovered high-pressure phase after pressure release, at ambient conditions. The numbers $1/x$ indicate the relative scale of the spectra. (*a*) The initial $2D$(T) polymeric phase. (*b*) The high-pressure phase of the polymer. (*c*) The main component among the pieces of the detonated sample identified as a mixture of the C_{60} monomer and dimer. (*d*) The diamond-like carbon phase identified among the pieces of the detonated sample

changes in the Raman intensity distribution and the high-pressure phase remains stable down to the ambient pressure. The bottom spectrum in Fig. 1*b* was recorded at 0.6 GPa, while the sample was recovered in air after disassembling the diamond anvil cell and tested again by means of micro-Raman probing. In Fig. 2, the Raman spectrum of the $2D$(T) polymer recorded at ambient conditions (Fig. 2*a*) is illustrated in comparison with that of the high-pressure phase of the recovered material (Fig. 2*b*). The spectra in Fig. 2 were recorded outside the diamond anvil cell, and it was therefore attainable to also measure the spectrum of each material in the frequency region of the T_{2g} mode of diamond. The Raman spectrum of the high-pressure

phase at ambient conditions is quite different from that of the initial $2D$(T) polymeric phase of C_{60}. The peak positions for the $2D$(T) polymer and those for the recovered high-pressure phase are shown in Table at ambient conditions.

The recovered high-pressure phase of the $2D$(T) polymer exhibits a metastable behavior. More specifically, after a time period of several days from the moment of its exposure to air, the recovered sample was detonated upon laser irradiation using the power 0.4 mW (objective: 100×) on the laser spot at the surface of the sample. The detonation is a rapid «explosive» process that was probably initiated by the thermal energy deposited by the probing laser beam; it results in a rapid relaxation of the built-in strain in the sample. We note that under these conditions, the laser power density on the sample is higher than the density reaching the sample inside the high-pressure cell due to the different optical systems used (different magnification factors and laser spot diameters). In addition, thermal dissipation conditions are different in the two cases, because the sample is surrounded by the pressure-transmitting medium in the cell. After the detonation, two phases were identified among the pieces of the recovered sample, characterized by their completely different Raman spectra presented in Figs. 2*c* and 2*d*. In Fig. 2*c*, the spectrum of the main part of the detonated sample is illustrated. This Raman spectrum is similar to that expected from a mixture consisting of dimers and monomers of C_{60} [1, 2, 14]. The presence of this phase in the detonated sample definitely proves that the C_{60} molecular cages are retained in the high-pressure phase of the $2D$(T) polymer. Finally, in Fig. 2*d*, the Raman spectrum of the phase that is a minority among the pieces of the detonated sample is given. As can be seen, the Raman spectrum of this phase is rather weak, consisting of two relatively broad peaks at 1342 and 1591 cm^{-1} (see Table). We have recorded the spectrum of this phase after the sample detonation but because the spectrum is too weak, we are not sure whether this phase was also present in the sample before its detonation, or even in the initial $2D$(T) polymer before the application of pressure. Fullerite phases having Raman spectra similar to that in Fig. 2*d* have been observed in C_{60} treated at the pressure 12.5 GPa and the temperature higher than 700 °C [32], as well as in C_{60} treated at the pressure 9.5 GPa and the temperature higher than 1500 °C [33]. These phases were characterized by X-ray and microhardness studies as disordered carbon phases having high density and hardness [32–34] and were attributed to the breakdown of C_{60} molecular cages and the formation of a cross-linked structure of graphite-like layers [33]. Indeed, the Raman spectra of these carbon phases, as well as the spectrum presented in Fig. 2*d*, are similar to that of the amorphous carbon containing a significant amount of sp^2 bonded carbon atoms [35] and to those of the microcrystalline graphite or diamond-like carbon films, mostly consisting of sp^3 hybridized carbon atoms [36, 37]. We therefore characterize the phase that is the minority among the pieces of the detonated sample as the diamond-like phase and we ascribe the respective Raman peaks of this phase at 1342 cm^{-1} and 1591 cm^{-1} (Fig. 2*d* and Table) to the D (diamond) and G (graphite) peaks of the microcrystalline graphite [38].

The obtained experimental data provide a strong indication that the $2D$(T) polymer of C_{60} undergoes a phase transition above 20 GPa. The transformation occurs via an intermediate state having a rather diffuse Raman spectrum, which characterizes a highly disordered pretransitional state of the material in the pressure near 4 GPa. The fact that the prominent Raman peaks of the high-pressure phase are related to the retention of the C_{60} cages in this phase is an indication that the new phase of the polymer can be related to a three-dimensional ($3D$) polymerization of C_{60}. The observed peculiarities in the pretransitional pressure range also support the assumption of a further pressure-induced polymerization, which is a solid-state chemical reaction rather than a structural phase transformation. The Raman spectrum of the high-pressure phase is dominated by a very strong Raman peak around 1842 cm^{-1}, which cannot be related to any internal vibrational mode of the C_{60} molecular cage. The strong Raman peaks ranged near 1600–1900 cm^{-1} in some chemical compounds of carbon are related to the stretching vibrations of isolated double C═C bonds [39]. In analogy to that, the strong peak at 1842 cm^{-1} can be attributed to the destruction of a number of double C═C bonds during further polymerization of the $2D$(T) polymer and to the appearance of some of the remaining ones as isolated C═C bonds in the $3D$ network of the C_{60} polymeric material. A more detailed analysis of the phonon modes and their pressure dependence in the initial $2D$(T) polymer and in the high-pressure phase are discussed in the next subsection.

3.2. Phonon modes

The pressure dependence of the Raman modes of the $2D$(T) polymer of C_{60} in the initial phase (squares)

Phonon frequencies, pressure coefficients, and the Grüneisen parameters for the initial $2D$(T) polymeric phase of C_{60}, the high-pressure phase, and pristine C_{60}. The phonon frequencies for the diamond-like carbon and dimeric C_{60} phases observed after the sample detonation are also included

Mode[a]	$2D$(T) polymeric C_{60}			High-pressure phase			
	ω_i, cm^{-1}	$\partial\omega_i/\partial P$, cm^{-1}/GPa[b]	γ_i	ω_i, cm^{-1}	$\partial\omega_i/\partial P$, cm^{-1}/GPa		γ_i
		$P <$ < 4 GPa			$P <$ < 10 GPa	$P >$ > 10 GPa	
$H_g(1)$	259	5.8	0.78	–	–		–
$H_g(1)$	282	2.3	0.264	297	0.3		0.047
$F_{2u}(1)$	363	−0.2	−0.019	391	−0.2		−0.024
$H_g(2)$	416	−0.1	−0.009	–	–		–
$H_g(2)$	432	0.6	0.049	442	0.6		0.064
$H_g(2)$	456	0.3	0.023	459	0.8		0.079
$A_g(1)$	487	4.5	0.322	–	–		–
$F_{1u}(1)$	–	–	–	–	–		–
$F_{2g}(1)$	536	1.4	0.091	540	0.6		0.052
$F_{1g}(1)$	563	1.4	0.087	554	1.3	0.8	0.111
$F_{1g}(1)$	588	0.8	0.047	571	1.8	0.9	0.148
$F_{1g}(1)$	–	–	–	634	2.7	0.9	0.201
$H_g(3)$	666	0.7	0.036	–	–	–	–
$H_g(3)$	683	2.3	0.118	688	1.4	1.0	0.096
$H_g(3)$	–	–	–	–	–	–	–
$H_g(4)$	748	−0.7	−0.033	738	1.9	1.3	0.121
$H_g(4)$	751[c]	–	–	–	–	–	–
$H_g(4)$	772	−1.2	−0.054	769	2.1	1.6	0.128
$H_g(4)$	773[c]	–	–	–	–	–	–
$H_g(4)$	–	–	–	826	2.4		0.137
$H_u(4)$	861	−0.6	−0.024	877	1.6		0.086
$H_u(4)$	–	–	–	902	2.1		0.109
$H_u(u)$	–	–	–	915	2.2		0.113
$G_g(2)$	955	4.5	0.164	961	3.0		0.147
$G_g(2)$	–	–	–	972	3.7		0.179
$F_{2u}(4)$	1041	4.2	0.141	1029	3.8		0.174
$F_{2u}(4)$	–	–	–	1064	2.8		0.124
$H_g(5)$	1107	4.8	0.151	–	–		–
$G_g(3)$	1178	6.7	0.198	–	–		–
$F_{2g}(3)$	1206	7.6	0.22	–	–		–
$H_g(6)$	–	–	–	–	–		–
$F_{2u}(5)$	–	–	–	–	–		–
$H_g(7)$	1403	6.6	0.164	–	–		–
$A_g(2)$	1448	6.1	0.147	1430	4.3		0.14
$F_{1g}(3)$	1464	7.6	0.181	–	–		–
$F_{2g}(4)$	1541	5.1	0.115	1509	3.9		0.119
$H_g(8)$	1572	5.9	0.131	1567	3.7		0.111
$G_g(6)$	1623	4.7	0.1	1647	4.1		0.117
$G_g(6)$	–	–	–	1842	3.5		0.089

Mode[a]	Pristine C_{60}			Dimer C_{60}	Diamond-like phase
	ω_i, cm^{-1}	$\partial\omega_i/\partial P$, cm^{-1}/GPa	γ_i	ω_i, cm^{-1}	ω_i, cm^{-1}
	0.4 GPa $< P <$ 2.4 GPa				
$H_g(1)$	272	3.2	0.165	266	–
$H_g(1)$	294	2.5	0.119	–	–
$F_{2u}(1)$	345	2.9	0.118	–	–
$H_g(2)$	389	−0.2	−0.007	–	–
$H_g(2)$	435	2.4	0.077	427	–
$H_g(2)$	454	1.4	0.043	–	–
$A_g(1)$	495	4.2	0.119	489	–
$F_{1u}(1)$	522	1.4	0.027	523	–
$F_{2g}(1)$	–	–	–	–	–
$F_{1g}(1)$	563	0.8	0.02	–	–
$F_{1g}(1)$	–	–	–	–	–
$F_{1g}(1)$	624	1.5	0.034	–	–
$H_g(3)$	–	–	–	–	–
$H_g(3)$	–	–	–	–	–
$H_g(3)$	710	−0.8	−0.016	704	–
$H_g(4)$	729	−2.9	−0.056	–	–
$H_g(4)$	755	−4.1	−0.078	–	–
$H_g(4)$	772	−2.7	−0.049	768	–
$H_g(4)$	–	–	–	–	–
$H_g(4)$	–	–	–	–	–
$H_u(4)$	–	–	–	847	841
$H_u(4)$	–	–	–	–	–
$H_u(4)$	–	–	–	–	915
$G_g(2)$	–	–	–	956	–
$G_g(2)$	–	–	–	–	–
$F_{2u}(4)$	–	–	–	–	–
$F_{2u}(4)$	–	–	–	–	–
$H_g(5)$	–	–	–	–	–
$G_g(3)$	–	–	–	–	–
$F_{2g}(3)$	–	–	–	–	–
$H_g(6)$	–	–	–	1239	–
$F_{2u}(5)$	–	–	–	1328	D1342
$H_g(7)$	1422	9.8	0.096	1420	–
$A_g(2)$	1467	5.5	0.053	1461	–
$F_{1g}(3)$	–	–	–	–	–
$F_{2g}(4)$	–	–	–	–	–
$H_g(8)$	1570	4.8	0.043	1566	G1591
$G_g(6)$	–	–	–	1624	–
$G_g(6)$	–	–	–	–	–

[a] The mode assignment refers to the irreducible representations of the icosahedral C_{60} molecule [40] and follows that in [14]; it is given here only for the initial phase of the $2D$(T) polymer and the «dimeric» C_{60} phase. [b] Data taken from [30]. [c] Frequency value at $P = 6$ GPa.

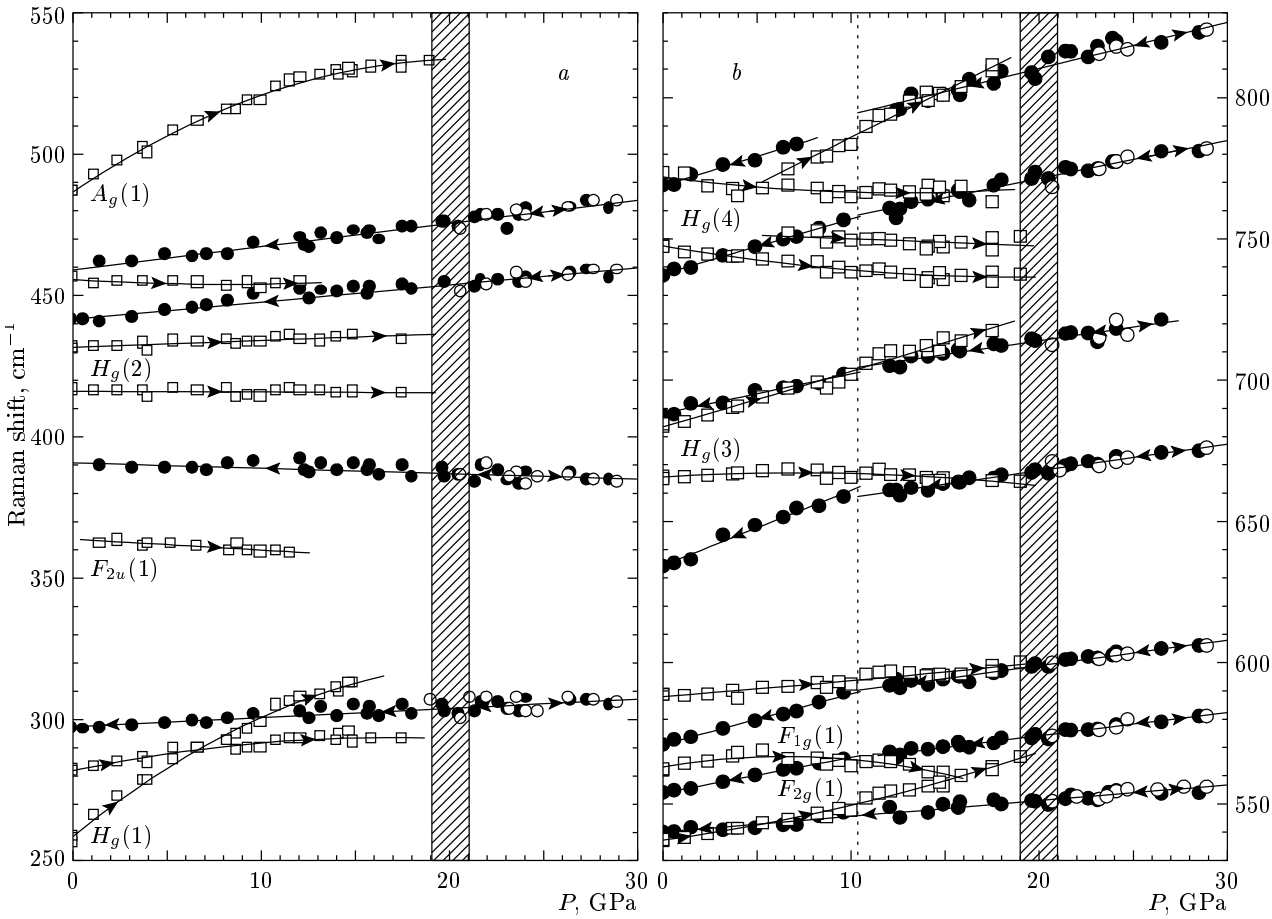

Fig. 3. The pressure dependence of the Raman modes of the $2D$(T) polymeric phase of C_{60} in the frequency regions 250–550 cm^{-1} (a) and 530–830 cm^{-1} (b). Squares and circles represent data taken for the $2D$(T) polymer in the initial and high-pressure phases, respectively. The open (solid) symbols denote data taken for increasing (decreasing) pressure runs. The shaded area near 20 GPa denotes the pressure range of the phase transformation. The dotted vertical line near 10.4 GPa in Fig. 3b denotes the pressure where changes in the slope of the pressure dependence occur during pressure decrease

and the high-pressure phase (circles) is shown in Figs. 3 and 4. The open (solid) symbols denote data taken for increasing (decreasing) pressure runs. Solid lines are drawn to guide the eye and arrows indicate the pressure increase or decrease. In these figures, the mode assignment refers to the irreducible representations of the parent C_{60} molecule (I_h symmetry) [40], following the notation in Ref. [14] in general, and is given here only for the initial $2D$(T) phase of the polymer. Table contains a compilation of the mode assignment (given for the initial $2D$(T) polymeric and the «dimeric» C_{60} phases), phonon frequencies ω_i, pressure coefficients $\partial\omega_i/\partial P$, and the corresponding Grüneisen parameters γ_i that in the present work are defined for the initial $2D$(T) polymeric and high-pressure phases. The Grüneisen parameters

$$\gamma_i = -\frac{\partial\omega_i/\omega_i}{\partial V/V} = \frac{B_0}{\omega_i^0}\frac{\partial\omega_i}{\partial P}$$

were calculated using the experimental data of the pressure coefficients $\partial\omega_i/\partial P$ for the phonon modes in both phases of the $2D$(T) polymer. The bulk modulus $B_0 = 34.8$ GPa for the initial $2D$(T) polymeric phase was taken from Ref. [19]. Because the experimental data are absent for this material, we have also used the theoretical value of the bulk modulus $B_0 = 47$ GPa [12] for the calculation of the Grüneisen parameters in the high-pressure phase. We note that the values of γ_i for the high-pressure phase are only an estimation because the real value of B_0 can differ from the theoretically predicted one. The appropriate data of the phonon mode frequencies of pristine C_{60}, their pressure coefficients and Grüneisen parameters calculated using the

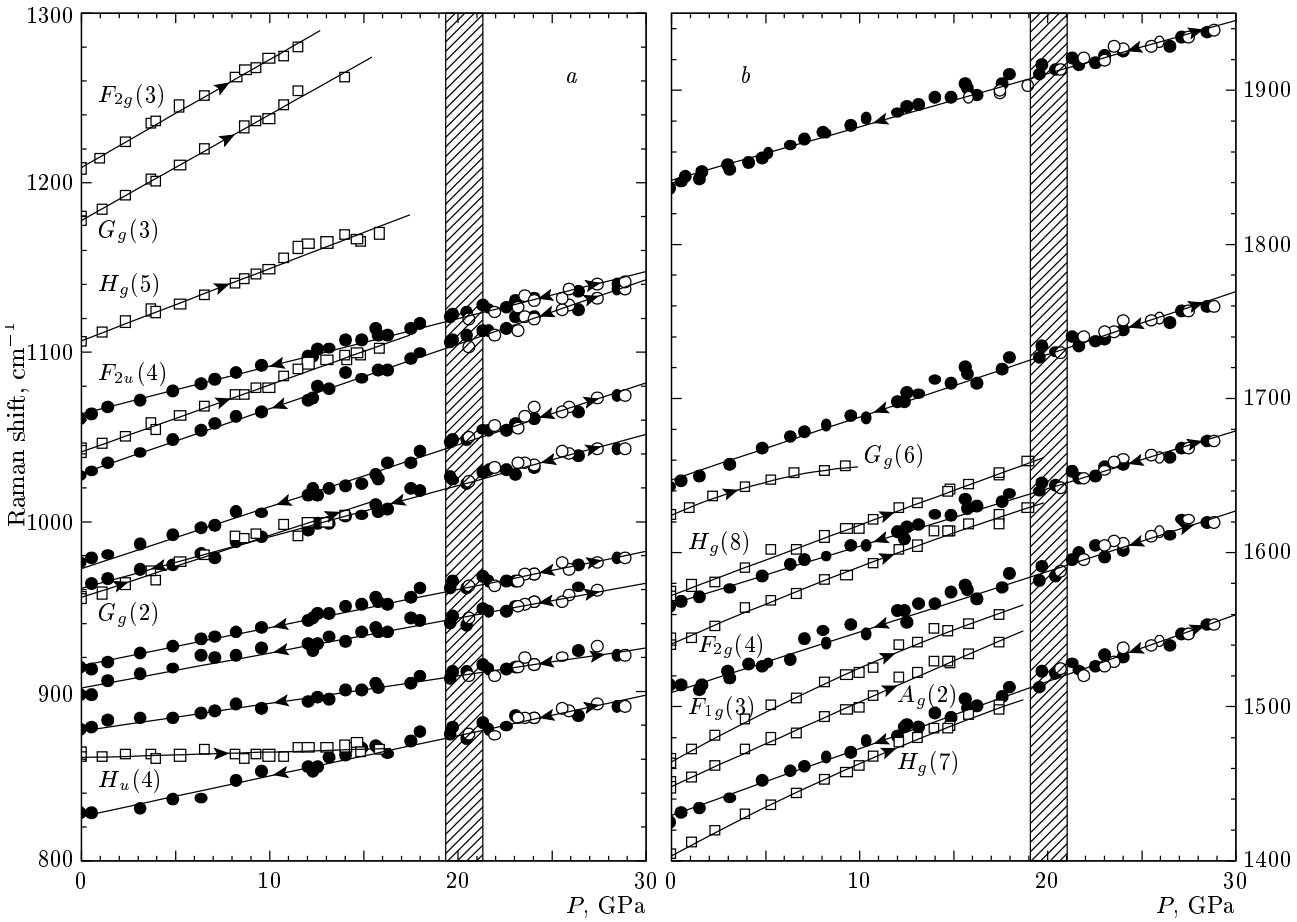

Fig. 4. The same as in Fig. 3 for C_{60} in frequency regions 800–1300 cm^{-1} (a) and 1400–1950 cm^{-1} (b)

bulk modulus $B_0 = 14.4$ GPa [41] are included in Table for comparison [42]. The last two columns in Table contain the phonon mode frequencies for the two phases (diamond-like and «dimeric» C_{60}) observed after the sample detonation at ambient conditions.

As can be seen from Figs. 3 and 4, all the Raman peaks of the initial $2D$(T) phase disappear in the pressure range 16 GPa $< P <$ 20 GPa, while the Raman peaks related to the high-pressure phase gradually appear and gain in intensity above 20 GPa (the shaded area in Figs. 3 and 4 indicates the pressure range of the transformation). It is also clear that the majority of the Raman modes of the high-pressure phase are related to those of the $2D$(T) polymer, showing that they originate from the C_{60} molecular cage vibrations. The nature of some phonon modes in the initial phase of the $2D$(T) polymer of C_{60}, in particular the Raman peak near 1040 cm^{-1}, is related to the covalent intermolecular bonding within the $2D$ polymeric layers [1, 14, 21]. More specifically, the peak near 1040 cm^{-1} is associated with the vibrations of the sp^3-like coordinated carbon atoms; the much lower frequency of this peak compared to that of the T_{2g} mode of diamond [28] can be attributed to the different lengths of the sp^3-like bonds in the $2D$(T) polymer (1.64 Å) and diamond (1.54 Å). In the recovered high-pressure phase, this mode appears to have two components with the frequencies 1029 and 1064 cm^{-1}. Assuming that the high-pressure phase is related to the formation of a $3D$ polymeric phase of C_{60} proposed by Okada et al. [12], we can associate these two Raman peaks with the existence of two types of sp^3-like coordinated carbon atoms with slightly different bond lengths.

Another important feature of the phonon spectrum of the high-pressure phase is the drastic changes in the region of the $A_g(2)$ pentagonal-pinch (PP) mode with respect to pristine C_{60} and its $2D$(T) polymeric phase. The PP-mode in pristine C_{60} is related to the in-phase stretching vibration of the five double C═C bonds originating in the vertices of each pentagon in the

fullerene molecular cage. The frequency of the PP-mode in the polymeric fullerenes decreases as the number of the polymeric covalent bonds per each molecular cage increases. Thus, the PP-mode in the Raman spectrum of the «dimeric» fullerene C_{120} is disposed around 1462 cm^{-1} (from 1469 cm^{-1} in pristine C_{60}), is then softened to 1457 cm^{-1} in $1D$(O), to 1449 cm^{-1} in $2D$(T), and further down to 1406 cm^{-1} in the $2D$(R) polymer [14]. The additional increase of the number of sp^3-like coordinated carbon atoms in the $3D$ polymer results in more drastic changes in the PP-mode region. Namely, five strong peaks appear in the Raman spectrum of the high-pressure phase, with the most intense of them located near 1842 cm^{-1}. The breakdown of a large number of double C═C bonds in the high-pressure phase therefore leads to quenching the PP-mode; as a result, a number of new Raman peaks appear that are possibly related to the stretching vibrations of the remaining isolated double C═C bonds. It is well known that the stretching vibrations of the isolated double C═C bonds are Raman-active and their frequencies range up to 2000 cm^{-1} [39].

The pressure dependence of the phonon frequencies of the $2D$(T) polymer shows a linear behavior for almost all modes and is absolutely reversible for pressures up to 12 GPa [30]. Nevertheless, two modes, $H_g(1)$ and $A_g(1)$, demonstrate a strong sublinear pressure dependence. The $A_g(1)$ mode is a «breathing» mode of the fullerene molecular cage and is associated with radial displacements in the atomic motions. To a large extent, the $H_g(1)$ mode is also related to the radial displacements of the carbon atoms. These two modes are therefore characterized by out-of-plane displacements of carbon atoms and in our opinion, their sublinear pressure dependence can be associated with the high anisotropy related to the Van der Waals intermolecular bonding of adjacent $2D$ polymeric layers and the covalent intermolecular bonding within the layers. Such a behavior is typical of the $2D$ polymeric phases of C_{60} and was recently also observed in the $2D$(R) polymer [20]. In addition, the $A_g(1)$ mode completely disappears at $P \geq 20$ GPa and is not present in the high-pressure phase. Such a behavior can be the result of the $3D$ polymeric bonding in the high-pressure phase, which quenches the «breathing» vibration of the fullerene molecular cage.

In the high-pressure phase, the frequencies of all the observed modes increase with increasing the pressure, except for the peak at 391 cm^{-1}, which shows a small negative pressure slope (see Table). The pressure coefficients $\partial\omega_i/\partial P$ of the Raman modes in the high-pressure phase range from -0.2 to 4.1 cm^{-1}/GPa, and the pressure slopes in the initial phase of the $2D$(T) polymer range from -1.2 to 7.6 cm^{-1}/GPa. At the same time, the pressure coefficients of the Raman modes in pristine C_{60} range from -4.1 to 9.8 cm^{-1}/GPa. These data agree with the fact that the polymerized materials become harder as the degree of polymerization increases [1, 12, 41]. It is interesting to note that the pressure coefficients of the Raman peaks at 1029 and 1064 cm^{-1}, associated with the sp^3-like coordinated carbon atoms, are comparable to that of the T_{2g} mode of the crystalline diamond (3.8, 2.8, and approximately 2.7 cm^{-1}/GPa, respectively) [43]. Finally, it is important to note that several Raman modes of the high-pressure phase, located in the frequency region 550–800 cm^{-1}, reveal changes in their pressure slopes to higher values as the pressure decreases below 10 GPa (see Table and the dotted line in Fig. 3*b*). These changes in the pressure slopes can be related to the theoretically predicted relaxation of the tetragonal lattice parameters in the high-pressure phase after the pressure release. As shown in [12], the lattice parameter a of the high-pressure phase at normal conditions is enlarged with respect to that of the initial $2D$(T) polymer from about 0.3 Å to 9.4 Å. We also think that the relaxation of the lattice parameter in the recovered high-pressure phase is responsible for the softening of the 1040 cm^{-1} mode in the initial $2D$(T) polymer to 1029 cm^{-1} in the new high-pressure phase (the low-frequency split component).

In Fig. 5, we show the correlation of the Grüneisen parameters γ_i to the phonon mode frequencies ω_i. The respective data for pristine C_{60}, for the initial phase of the $2D$(T) polymer of C_{60}, and for its high-pressure phase are represented by open triangles, circles, and squares. The single solid star indicates the Grüneisen parameter of the T_{2g} mode of diamond, which is as large as 0.895. The values of γ_i for the three materials investigated vary between -0.078 and 0.78; in general, they behave similarly to frequency, exhibiting two maxima near 600 and 1300 cm^{-1} and two minima near 400 and 750 cm^{-1}. Both minima are related to soft intramolecular modes and are characterized by negative values of γ_i, indicating the possible instability of the C_{60} molecular cage with respect to the atomic displacements related to these modes. We note that the polymerization of pristine C_{60} leads to a deformation of the fullerene molecular cage, which in particular results in the reduction of the number of modes with negative values of γ_i. This reduction becomes more significant in the fullerenes with a higher degree of polymerization. Another interesting observation is that the maximum in the frequency dependence of the Grüneisen parameters

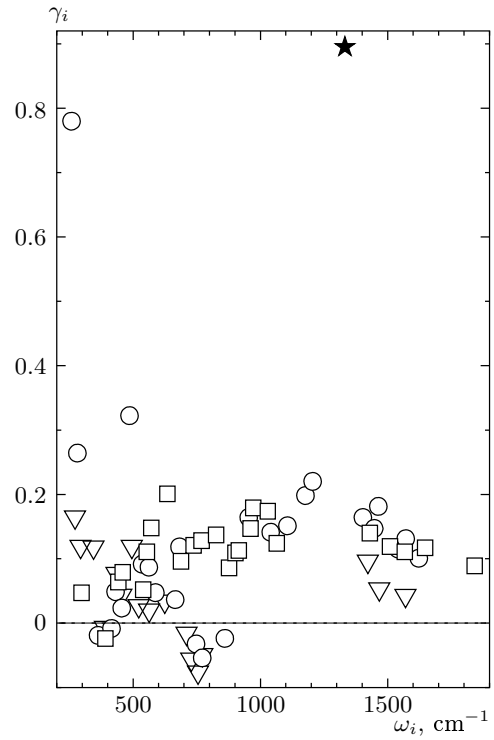

Fig. 5. Grüneisen parameters for the various modes of pristine C_{60} (triangles), the initial $2D$(T) polymeric phase (circles), and its high-pressure phase (squares). The solid star indicates the Grüneisen parameter of the T_{2g} mode of diamond at 1332 cm^{-1}

around the T_{2g} mode of diamond at 1332 cm^{-1} is more pronounced for the polymerized fullerenes. This implies, in particular, that the appropriate phonon modes of the polymeric fullerenes involve atomic motions of the sp^3-like coordinated carbon atoms as in the case of the T_{2g} mode of diamond.

We finally consider the very large values of γ_i for the $H_g(1)$ and $A_g(1)$ modes in the $2D$(T) polymer. These modes are greatly affected by the Van der Waals interaction between the $2D$ polymeric layers due to the out-of-plane nature of the relevant atomic motions. In addition, the deformation of the fullerene molecular cage related to the additional $3D$ polymeric bonding also contributes to the large values of γ_i for these two modes.

3.3. Photoluminescence and electronic spectrum

The photoluminescence spectra of the $2D$(T) polymeric phase of C_{60}, for pressures up to 3 GPa and room temperature, recorded for various increasing and decreasing pressure runs, are shown in Fig. 6*a* and Fig. 6*b*, respectively. The inset in Fig. 6*b* shows the photoluminescence spectrum of the $2D$(T) polymer in comparison with the photoluminescence spectra of pristine C_{60} at room temperature and at 10 K [44]. The fluorescence intensity in the $2D$(T) polymer is noticeably higher than in pristine C_{60}. This is related to the fact that the lowest excited singlet state of the C_{60} molecule has the $^1T_{1g}$ symmetry and optical transitions to this state are dipole forbidden [45, 46]. In solutions, the fluorescence of C_{60} is related to the vibronically assisted Herzberg–Teller transitions [47], whereas in the solid state, the additional increase of the fluorescence quantum yield is related to the violation of the symmetry restrictions by the presence of crystal impurities and defects. The polymerization reduces the molecular symmetry from I_h in pristine C_{60} to D_{2h} in the $2D$(T) polymer and eliminates the symmetry restrictions leading to an essential increase in the photoluminescence quantum yield.

As can be seen from the inset in Fig. 6*b*, the photoluminescence spectrum of the $2D$(T) polymer differs from that of pristine C_{60} in both the intensity distribution and the onset of luminescence. The well-structured low-temperature photoluminescence spectrum of the high-quality single crystals of C_{60} is mainly related to excitons localized on defects or impurity levels [44, 48]. On the contrary, the photoluminescence spectrum of C_{60} at room temperature consists of two broad bands and is related to the vibronically assisted transitions from the lowest singlet $^1T_{1g}$ level (the first band at about 1.665 eV). The most intense bands in the photoluminescence spectrum of the $2D$(T) polymer located near 1.533 eV and 1.435 eV are related to the fluorescence of the host $2D$(T) polymer, while the weak shoulders at higher energies (near 1.748 eV and 1.661 eV) originate from the impurity phase of $2D$(R) that is present in the $2D$ polymeric samples [49]. We note that the very sharp lines in Figs. 6*a* and 6*b* near 1.785 eV are related to the R_1 and R_2 luminescence bands of the ruby chips used for pressure calibration [27].

The increase of pressure results in a gradual shift of the photoluminescence spectrum to lower energies, lowering and redistribution of the fluorescence intensity. These changes are absolutely reversible in the pressure range investigated ($P \leq 4$ GPa), as can be seen in Fig. 6. The integrated intensity of the photoluminescence spectrum rapidly decreases with the increase of pressure and recovers its strength nearly to its initial value after the total pressure release.

The pressure dependence of the band positions in the photoluminescence spectrum of the $2D$(T) poly-

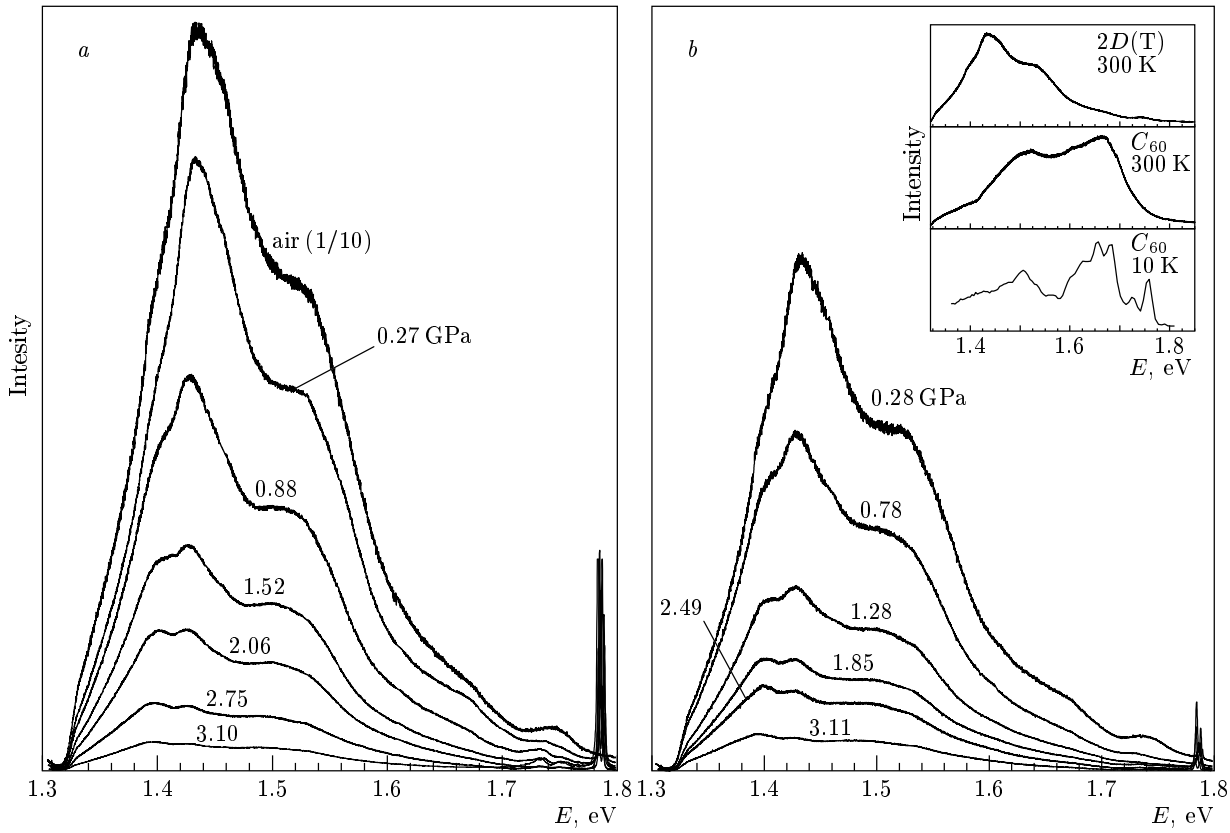

Fig. 6. Photoluminescence spectra of the $2D$(T) polymer at 300 K and various pressures for the increasing (a) and decreasing (b) pressure runs. Inset: photoluminescence spectra of pristine C_{60} at 10 K and 300 K in comparison with that of the $2D$(T) polymer at room temperature

mer is shown in Fig. 7. The open (closed) triangles, squares, circles, and diamonds are related to the bands near 1.748, 1.661, 1.533, and 1.435 eV for the upstroke (downstroke) pressure runs, respectively. The open hexagons show the pressure dependence of the first peak in the fluorescence spectrum of pristine C_{60} [44] and are included in the figure for comparison. The pressure-induced shift $\partial E/\partial P$ for the photoluminescence bands of the $2D$(T) polymer varies from -9 meV/GPa to -17 meV/GPa, whereas the corresponding value for pristine C_{60} is equal to -78 meV/GPa. The large difference in $\partial E/\partial P$ leads to the intersection of the pressure dependences for the $2D$(T) polymer (circles) and pristine C_{60} (hexagons) near 1.9 GPa, which is close to 2.2 GPa used in the HPHT treatment procedure for the production of the $2D$(T) polymer. This implies that the fluorescence onset in the $2D$(T) polymer is shifted to lower energies mainly because of the decrease of the intermolecular distances caused by the formation of the polymer. On the contrary, the deformation of the C_{60} cage in the polymer, which leads to the lowering of molecular symmetry, does not essentially affect the shift of the electronic spectrum.

We can calculate the deformation potential

$$D = \frac{\partial E_g}{\partial \ln(V_0/V)} = -B_0 \frac{\partial E_g}{\partial P},$$

where E_g is the direct gap and B_0 is the bulk modulus of the material, using the experimental data concerning the pressure-induced shift of the photoluminescence bands, $\partial E/\partial P$, obtained for both materials. Taking into account that the position of the first band in the photoluminescence spectrum coincides with the direct gap (in the case of vibronically-assisted transitions, it differs from the phonon energy), we obtain $D = 0.42$ eV and $D = 1.09$ eV for the $2D$(T) polymer and pristine C_{60}, respectively. It is interesting to note that a noticeable increase of the bulk modulus in the $2D$(T) polymer compared to pristine C_{60} does not result in a similar increase of the deformation potential due to the lowering of the pressure-induced shift of the electronic spectrum.

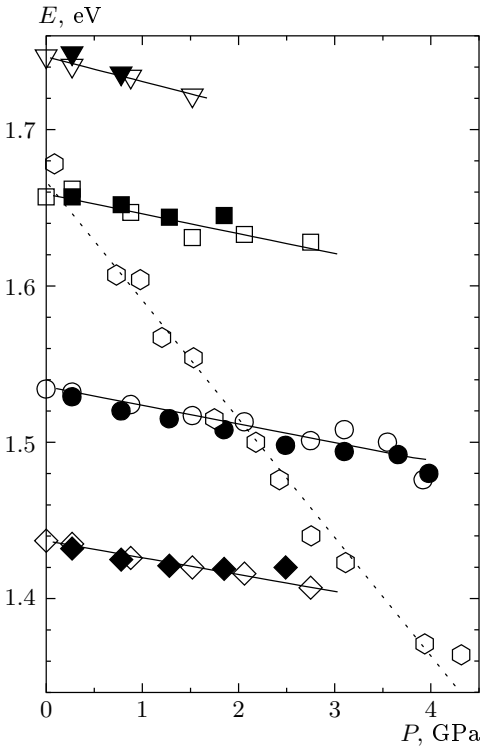

Fig. 7. Pressure dependence of the fluorescence bands in the photoluminescence spectra of the $2D$(T) polymer and pristine C_{60}. Open (closed) triangles, squares, circles, and diamonds show various bands of the $2D$(T) polymer for the increasing (decreasing) pressure runs. Open hexagons show the first fluorescence band of pristine C_{60} for an upstroke pressure run

4. CONCLUSIONS

The Raman scattering data under high hydrostatic pressure show that an irreversible transformation occurs in the $2D$(T) polymeric phase of C_{60} above 20 GPa. The new phase is preceded by a pretransitional state characterized by diffuse Raman peaks. The spectrum of the high-pressure phase remains intense and well resolved at pressures as high as 30 GPa. The phonon modes of the high-pressure phase, especially in the high-energy region, are noticeably different from those of the initial $2D$(T) polymer; nevertheless, they can be tracked back to the phonon modes related to the fullerene molecular cage. The recovered high-pressure phase is metastable and detonates under laser irradiation. The main part of the detonated sample is a mixture of monomeric and dimeric C_{60}, showing that the fullerene molecular cages are retained in the high-pressure phase. The high-pressure phase seems to be related to further creation of covalent bonds between molecules belonging to the adjacent polymeric layers in accordance with the theoretically predicted $3D$ polymerization of the $2D$(T) C_{60} polymer at 20.2 GPa [12]. Our Raman experiments reveal that the $3D$ polymeric C_{60} resulting from the application of high pressure on the $2D$(T) polymer is not related to the previously observed ultrahard fullerite phases [1, 8, 9]. The electronic spectrum of the $2D$(T) polymer is noticeably different from that of pristine C_{60}. This difference is related both to the deformation of the fullerene molecular cage caused by the polymerization of material and to the decrease of the in-plane intermolecular distances in the $2D$(T) polymer.

The support by the General Secretariat for Research and Technology, Greece, is gratefully acknowledged. One of the authors (K. P. M.) acknowledges the support by the Russian State Research Program «Physical properties of carbon-based nanostructures and development of new electronic devices». Another author (B. S.) acknowledges the support from the Swedish Research Councils for Natural Sciences (NFR) and Engineering Sciences (TFR).

The authors thank A. Soldatov and T. Wägberg for help with preparation and characterization of the $2D$(T) polymer of C_{60}.

REFERENCES

1. B. Sundqvist, Adv. Phys. **48**, 1 (1999).
2. A. M. Rao, P. Zhou, K.-A. Wang et al., Science **259**, 955 (1993).
3. P. W. Stephens, G. Bortel, G. Faigel et al., Nature (London) **370**, 636 (1994).
4. K. Prassides, K. Vavekis, K. Kordatos et al., J. Amer. Chem. Soc. **119**, 834 (1997).
5. Y. Iwasa, T. Arima, R. M. Fleming et al., Science **264**, 1570 (1994).
6. M. Nunez-Regueiro, L. Marques, J.-L. Hodeau et al., Phys. Rev. Lett. **74**, 278 (1995).
7. V. V. Brazhkin, A. G. Lyapin, and S. V. Popova, Pis'ma Zh. Eksp. Teor. Fiz. **64**, 755 (1996) [JETP Lett. **64**, 802 (1996)].
8. V. D. Blank, M. Yu. Popov, S. G. Buga et al., Phys. Lett. A **188**, 281 (1994).
9. V. D. Blank, S. G. Buga, G. A. Dubitsky et al., Carbon **36**, 319 (1998).

10. L. Marques, M. Mezouar, J.-L. Hodeau et al., Science **283**, 1720 (1999).

11. L. A Chernozatonskii, N. R. Serebryanaya, and B. N. Mavrin, Chem. Phys. Lett. **316**, 199 (2000).

12. S. Okada, S. Saito, and A. Oshiyama, Phys. Rev. Lett. **83**, 1986 (1999).

13. E. Burgos, E. Halac, R. Weht et al., Phys. Rev. Lett. **85**, 2328 (2000).

14. V. A. Davydov, L. S. Kashevarova, A. V. Rakhmanina et al., Phys. Rev. B **61**, 11936 (2000).

15. G. A. Kourouklis, S. Ves, and K. P. Meletov, Physica B **265**, 214 (1999).

16. J. Arvanitidis, K. Papagelis, I. Tsilika et al., Physica B **265**, 234 (1999).

17. K. P. Meletov, J. Arvanitidis, I. Tsilika, S. Assimopoulos, G. A. Kourouklis, S. Ves, A. Soldatov, and K. Prassides, Phys. Rev. B **63**, 054106 (2001).

18. K. P. Meletov, S. Assimopoulos, I. Tsilika et al., Chem. Phys. Lett. **341**, 435 (2001).

19. J. M. Leger, J. Haines, V. A. Davydov, and V. Agafonov, Sol. St. Comm. **121**, 241 (2002).

20. K. P. Meletov, J. Arvanitidis, G. A. Kourouklis et al., submitted to Chem. Phys. Lett. (2002).

21. T. Wågberg, A. Soldatov, and B. Sundqvist, unpublished.

22. R. Moret, P. Launois, T. Wågberg et al., Eur. J. Phys. B **15**, 253 (2000).

23. K. P. Meletov, E. Liarokapis, J. Arvanitidis et al., Chem. Phys. Lett. **290**, 125 (1998).

24. P.-A. Persson, P. Jacobsson, S. Stafstrom et al., Europhys. Lett. **49**, 631 (2000).

25. P.-A. Persson, U. Edlund, P. Jacobsson et al., Chem. Phys. Lett. **258**, 540 (1996).

26. A. Jayaraman, Rev. Sci. Instr. **57**, 1013 (1986).

27. D. Barnett, S. Block, and G. J. Piermarini, Rev. Sci. Instr. **44**, 1 (1973).

28. S. A. Solin and A. K. Ramdas, Phys. Rev. B **1**, 1687 (1970).

29. V. A. Davydov, L. S. Kashevarova, A. V. Rakhmanina et al., Phys. Rev. B **58**, 14786 (1998).

30. J. Arvanitidis, K. P. Meletov, K. Papagelis et al., J. Chem. Phys. **114**, 9099 (2001).

31. K. P. Meletov, D. Christofilos, S. Ves et al., Phys. Rev. B **52**, 10090 (1995).

32. V. V. Brazhkin, A. G. Lyapin, S. V. Popova et al., Phys. Rev. B **56**, 11465 (1997).

33. V. D. Blank, S. G. Buga, N. R. Serebryanaya et al., Carbon **36**, 665 (1998).

34. V. V. Brazhkin, A. G. Lyapin, S. V. Popova et al., J. Appl. Phys. **84**, 219 (1998).

35. M. Weiler, S. Sattel, T. Giessen et al., Phys. Rev. B **53**, 1594 (1996).

36. R. J. Nemanich and S. A. Solin, Phys. Rev. B **20**, 392 (1979).

37. R. E. Shroder, R. J. Nemanich, and J. T. Glass, Phys. Rev. B **41**, 3738 (1990).

38. M. S. Dresselhaus, M. A. Pimenta, P. C. Eklund et al., in *Raman Scattering in Material Science*, ed. by W. H. Weber and R. Merlin, Springer, Berlin (2000), p. 314.

39. D. A. Long, *Raman Spectroscopy*, McGraw-Hill, London (1976), p. 158.

40. M. C. Martin, X. Du, J. Kwon, and L. Mihaly, Phys. Rev. B **50**, 173 (1994).

41. J. Haines and J. M. Leger, Sol. St. Comm. **90**, 361 (1994).

42. K. P. Meletov, G. Kourouklis, D. Christofilos et al., Zh. Eksp. Teor. Fiz. **108**, 1456 (1995) [JETP **81**, 798 (1995)].

43. A. F. Goncharov, I. N. Makarenko, and S. M. Stishov, Pis'ma Zh. Eksp. Teor. Fiz. **41**, 150 (1985) [JETP Lett. **41**, 184 (1985)].

44. K. P. Meletov and V. D. Negrii, Pis'ma Zh. Eksp. Teor. Fiz. **68**, 234 (1998) [JETP Lett. **68**, 248 (1998)].

45. F. Negri, G. Orlandi, and F. Zerbetto, Chem. Phys. Lett. **144**, 31 (1988).

46. F. Negri, G. Orlandi, and F. Zerbetto, J. Chem. Phys. **97**, 6496 (1992).

47. G. Herzberg and E. Teller, Z. Phys. Chem. B **21**, 410 (1933).

48. W. Guss, J. Feldman, E. O. Gobel et al., Phys. Rev. Lett. **72**, 2644 (1994).

49. K. P. Meletov, S. Assimopoulos, and G. A. Kourouklis, unpublished.